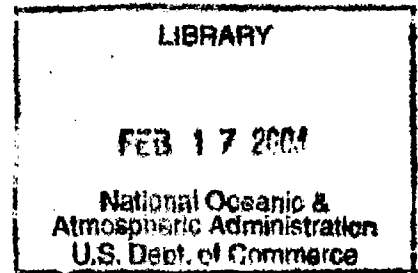


Technical Memorandum No. 8

U.S. Joint Numerical Weather Prediction Unit

Results of 24-hour barotropic
forecasts for the 100 mb pressure surface.



Geirmundur Arnason
U. S. Weather Bureau



RAREBOOK
QC
996
.T33
no. 8

Oct. 14, 1955

90333

National Oceanic and Atmospheric Administration

U.S. Joint Numerical Weather Prediction Unit

ERRATA NOTICE

One or more conditions of the original document may affect the quality of the image, such as:

Discolored pages

Faded or light ink

Binding intrudes into the text

This has been a co-operative project between the NOAA Central Library, National Center for Environmental Prediction and the U.S. Air Force. This project includes the imaging of the full text of each document. To view the original documents, please contact the NOAA Central Library in Silver Spring, MD at (301) 713-2607 x124 or www.reference@nodc.noaa.gov.

LASON

Imaging Contractor

12200 Kiln Court

Beltsville, MD 20704-1387

April 13, 2004

Observations show that variation in the static stability is, on the whole, considerably smaller in the stratosphere than in the troposphere. Moreover, it is known that the horizontal velocity divergence is closely related to time and space variation in the static stability and in such a way that small variation corresponds to small divergence. Inasmuch as the divergence term in the vorticity equation is omitted in performing the so-called barotropic forecasts, one is lead to conclude that the stratosphere is likely to be a preferred region for successful forecasts of this kind.

This is considered at some length in an appendix to this note. The conclusion is reached, that the horizontal divergence is particularly small in the stratosphere and that consequently the absolute vorticity remains approximately conservative for a period of 24 hours.

These considerations as well as the well established usefulness of 500 mb barotropic forecasts initiated the task of carrying out 24 hour barotropic forecasts for the 100 mb surface for 30 consecutive days of January 1953. The synoptic charts had been analysed by the Analysis Section of the Numerical Prediction Project at Geophysics Research Directorate (referred to as GRD below), Cambridge, Mass., and tabulated height values for grid points were kindly made available to JNWP. The grid and the area of verification, shown in fig. 1, are the same as those used at GRD for their barotropic 500 mb (as well as thermotropic 1000 and 500 mb) forecasts for the same period (Jan. 1953). The details of the GRD forecasting procedure were purposely copied, as the goal was essentially to compare the skill of the 100 mb forecasts with the skill of those for the 500 mb. For practical reasons, one deviation was made from the GRD procedure; this was in the use of boundary conditions. At GRD $1/24$ of the observed 24 hour change centered at the initial instant was applied to the boundaries, whereas $1/24$ of the uncentered 24 hour forward change was used in connection with the 100 mb forecasts. This had to be done since, as a rule, the 15Z data were not needed for the forecasts and, therefore, not available on punched cards. Although the boundary values do not directly enter the verification, the difference in the applied boundary conditions will influence the results. There are indications that the

boundary conditions applied to the 100 mb forecasts may have been slightly more favourable for the results than those used for the 500 mb barotropic forecasts [2].

As for other details in the preparation of the 100 mb forecasts, the following are mentioned:

1. The mesh-size is approximately $2\frac{1}{2}$ degrees ^{of} latitude, and the grid is 18×23 gridpoints covering an area shown in fig. 1.
2. For the computations of the finite difference form of the Laplacian of the pressure heights a 5-point scheme was used where the four points surrounding the central point were four mesh-sizes apart. This gives a smoother (and somewhat weaker) vorticity field than the conventional scheme where the surrounding points are two mesh sizes apart.
3. The time step used was one hour.

Further details of the forecasting procedure may be found in the GRD-report on their 500 mb forecasts [1].

As a measure of the performance level of the 100 mb forecasts, correlation coefficients (R), root mean square of errors (σ_E), root mean squares of observed (σ_O) and predicted (σ_F) height changes were computed as well as the ratios σ_E/σ_O . These statistical quantities were selected mainly in order to facilitate comparison with the 60 24-hour barotropic 500 mb forecasts made at GRD.

Altogether 34 100 mb forecasts were run. Of these 30 were based on the 03Z data for Jan. 1-30, and 4 based on the 15Z data for Jan. 6, 7, 27, and 28. The results are shown in table 1. A comparison between the quantities R , σ_E , σ_O , and σ_E/σ_O for the 100 and 500 mb forecasts is given in the graphs of fig. 2, and the main results may be summarized as follows:

1. The mean correlation coefficients as well as the mean σ_F 's are practically the same for the two series of 34 100 mb forecasts and 60 500 mb forecasts, 0.73, 208 ft and 0.73, 228 ft respectively. This result did not change appreciably when all the 15Z forecasts were excluded.

2. The observed 24 hr changes at 100 mb were on the average $\frac{2}{3}$ of those at 500 mb, the respective figures are 199 ft and 293 ft. As a result the ratio $\frac{\sigma_E}{\sigma_O}$ was larger at 100 mb than at 500 mb. The respective means are 1.08 and 0.80.
3. There did not appear to be any systematic difference between σ_O and σ_F at 100 mb.

As regards details, attention is drawn to the rough indication of a 12-24 hour phase lag of the 100 mb R-curve compared with that of the 500 mb. An explanation is not attempted here since the synoptic situations were not studied although a possible explanation might be the upward propagation of low-level cyclogenesis. Another detail is the uniform sign of the observed height changes over the entire area of verification on Jan. 4, 8, and 11.

Table I. 100 mb forecasts (24 hours)

Jan. 1953	R	σ_E	σ_O	σ_F	$\frac{\sigma_E}{\sigma_O}$	
1 03Z	.66	18	16	15	1.13	
2 03Z	.84	18	18	20	1.00	
3 03Z	.84	12	15	14	0.80	
4 03Z	.45	22	18	10	1.22	
5 03Z	.82	16	17	21	0.94	
6 03Z	.88	16	18	21	0.89	
6 15Z	.89	19	21	21	0.90	
7 03Z	.42	37	25	17	1.48	
7 15Z	.72	28	37	26	0.76	
8 03Z	.28	37	32	20	1.16	
9 03Z	.76	16	17	16	0.94	
10 03Z	.70	22	17	15	1.29	
11 03Z	.18	25	21	14	1.19	
12 03Z	.77	19	19	19	1.00	
13 03Z	.80	30	18	29	1.67	
14 03Z	.91	14	22	24	0.64	
15 03Z	.63	24	12	20	2.00	
16 03Z	.78	17	17	10	1.00	
17 03Z	.77	16	16	15	1.00	

σ in tens of feet

Table I (continued)

Jan. 1953	R	σ_E	σ_o	σ_F	σ_E/σ_o
18 03Z	.91	14	22	21	0.64
19 03Z	.73	19	19	14	1.00
20 03Z	.57	27	19	22	1.42
21 03Z	.94	15	27	28	0.56
22 03Z	.87	15	15	18	1.00
23 03Z	.73	15	13	17	1.15
24 03Z	.90	15	17	17	0.88
25 03Z	.89	16	22	21	0.73
26 03Z	.66	26	19	22	1.37
27 03Z	.74	29	26	19	1.12
27 15Z	.68	22	22	18	1.00
28 03Z	.85	22	28	20	0.79
28 15Z	.81	26	21	15	1.24
29 03Z	.68	22	14	21	1.57
30 03Z	.85	19	17	16	1.12
Mean	.73	20.0	19.9	18.3	1.03

Appendix. Remarks on the gross-features of the vertical distribution of the horizontal velocity divergence.

When differentiated with respect to pressure, the adiabatic equation

$$(1) \frac{\partial \ln \theta}{\partial t} + \mathbf{v} \cdot \nabla \ln \theta + \omega \frac{\partial \ln \theta}{\partial p} = 0$$

leads to the following expression for $\frac{\partial \omega}{\partial p}$:

$$(2) \frac{\partial \omega}{\partial p} = -\frac{1}{\Gamma} \frac{\partial \Gamma}{\partial t} - \frac{\partial \Psi}{\partial p} \cdot \nabla \ln \theta$$

Notations used here are conventional; θ is the potential temperature (dry air) and Γ is given by:

$$(3) \Gamma = \frac{\partial \ln \theta}{\partial p} = -\frac{s}{p}, \text{ where}$$

$$(4) s = \frac{R}{g} \left(\frac{\partial \Gamma}{\partial p} + \frac{\partial \Gamma}{\partial z} \right)$$

It is now assumed that the wind is approximately geostrophic so that the last term in (2) may be omitted. Moreover, we substitute for ω from (3) into (2) which then takes the form

$$(5) \quad -\frac{\partial \omega}{\partial p} = \frac{1}{s} \frac{ds}{dt} - \frac{1}{p} \frac{dp}{dt} = \frac{1}{s} \frac{Ds}{Dt} - \frac{\omega}{p} = \frac{1}{s} \frac{Ds}{Dt} - \frac{\omega}{p} \left(1 + \frac{H}{s} \frac{\partial s}{\partial z}\right)$$

where $\frac{D}{Dt} = \frac{\partial}{\partial t} + \mathbf{V} \cdot \nabla$ and $H = \frac{RT}{g}$

By definition:

$$\omega = \frac{dp}{dt} \approx -\frac{p}{H} \frac{dz}{dt} = -\frac{p}{H} W$$

Substitution for ω into (5) gives:

$$(6) \quad -\frac{\partial \omega}{\partial p} = \frac{1}{s} \frac{Ds}{Dt} + \frac{1}{H} \left(1 + \frac{H}{s} \frac{\partial s}{\partial z}\right) \cdot W$$

We refer to the fact that $\frac{\partial \omega}{\partial p}$ is proportional to the horizontal velocity divergence and that Eq. (6) therefore shows that this quantity is closely related to the time and space variation of the static stability, s , as defined by Eq. (4). Certain information regarding the gross-features of the vertical distribution of the divergence may therefore be inferred from what is known about the field of static stability. Admittedly, our knowledge of this quantity is limited by the fact that charts of static stability are not prepared on a routine basis and normals are available only for the layer 1000 - 500 mb (3). Yet, observations would seem to support the following statements:

1. The combined time-space derivative $\frac{1}{s} \frac{Ds}{Dt}$ has in general two maxima, one somewhere in the lower half of the troposphere and another within the transition zone between the troposphere and the stratosphere. It has a relative minimum approximately between 600 and 400 mb and an absolute minimum in the stratosphere.

2. Whereas the variation of s with increasing height is quite irregular below around 600 mb, it generally decreases with increasing height between this level and the transition zone between the troposphere and the stratosphere. In the transition zone, however, there is an increase - in general quite considerable - in s with increasing height. In the stratosphere, variation with height is small and irregular.

To the extent $\text{div } \mathbf{V}$ depends on the first term on the right-hand

side of (6), the main features of the div \mathbf{v} - distribution along the vertical are already sketched under 1. above. The occurrence of the vertical velocity in the second right-hand term of (6) complicates the estimate of this term since something has to be assumed about the variation with height of this quantity. It is frequently assumed that W has a maximum near the middle or in the upper part of the troposphere, and it is generally assumed that it decreases from troposphere to stratosphere because of the increase in static stability. We will not stretch this point any further but rather investigate the proportionality factor $1 + \frac{H}{s} \frac{\partial s}{\partial z}$ which as we shall see, is quite sensitive to variation with height in the static stability. To this end we put $\frac{H}{s} \frac{\partial s}{\partial z}$ on the following form, utilizing Eq. (4):

$$(7) \quad \frac{H}{s} \frac{\partial s}{\partial z} = \frac{H}{g/C_p + \frac{\partial T}{\partial z}} \frac{\partial^2 T}{\partial z^2} = - \frac{H}{10-K} \frac{\Delta K}{\partial z} = - \frac{H}{1000} \cdot \frac{\Delta K}{10-K}$$

where $K = - \frac{\partial T}{\partial z} \cdot 10^3$, i.e. the lapse in temperature per kilometer, and ΔK is the increase in K per kilometer. Fig. 3 shows the value of ΔK , as a function of K , for which $1 + \frac{H}{s} \frac{\partial s}{\partial z}$ is zero. The solid line corresponds to $6.4 \cdot 10^3$ m, the broken one to $H = 7.1 \cdot 10^3$ m, the dash-dotted line to $H = 8.0 \cdot 10^3$ m representing roughly the conditions in the lower, middle and upper part (as well as the stratosphere) of the troposphere.

Values of ΔK well in excess of those required to make the last term in (6) zero occur frequently in the atmosphere. Because of the prevailing values of K and ΔK in the middle and upper troposphere, the magnitude of $1 + \frac{H}{s} \frac{\partial s}{\partial z}$ tends to be smaller here than below and in the transition zone between troposphere and stratosphere. This piece of information regarding the typical distribution of static stability with height together with the picture of the vertical velocity distribution sketched above, seems to indicate the whereas the second term in Eq. (6) may vary irregularly in the troposphere, it is comparatively small in the stratosphere. The order of magnitude of this term ranges probably from 10^{-6} in the stratosphere to 10^{-5} in the troposphere and is not negligible in comparison with the first term in Eq. (6).

In summary, the following gross-features of the distribution of the horizontal velocity divergence stand out as being plausible in view of the discussion above:

The horizontal velocity divergence is in general smaller in the stratosphere than in the troposphere. It has a relative maximum in the transition zone between troposphere and stratosphere and another in the lower half of the

troposphere. In the layer 600-400 mb it is comparatively weak.

Since the so-called barotropic forecasts neglect the divergence term in the vorticity equation

$$(8) \quad \frac{1}{\eta} \frac{D\eta}{Dt} + \text{div } \Psi = 0$$

one may expect such forecasts to be more successful at one level than another and in particular would the stratosphere seem to be preferred region in this respect. The time intervals which may be successfully spanned by a barotropic forecast is determined by the magnitude of $\text{div } \Psi$. In the stratosphere, the first term in Eq. (6) is of the order of magnitude 10^{-6} sec^{-1} and the same applies to the second one, provided W does not exceed $1-2 \text{ cm/sec}$, which seems likely. Let us assume, that a barotropic forecast may be considered useful if $\frac{\Delta\eta}{\eta}$ does not exceed 25 %, where $\Delta\eta$ is the actual change in vorticity during the forecast period and η is the absolute vorticity at the initial time. In view of Eq. (8) this requires that $|\text{div } \Psi| \Delta t \leq 0.25$, which for $\Delta t = 24 \text{ hours}$ gives $|\text{div } \Psi| \leq 0.3 \cdot 10^{-5} \text{ sec}^{-1}$. There are reasons to believe that the horizontal divergence of the stratosphere may fulfill this requirement.

References

1. Report of Progress for the Period 15 Feb. 1954-15 August 1954; Joint GRD-AWS Numerical Prediction Project. Air Force Cambridge Research Center, Cambridge, Mass., Aug. 15, 1954.
2. White, R. M., and Cooley, D.C.: A Test of the Feasibility of Extended Forecasting by Numerical Techniques. Air Force Cambridge Research Center, Cambridge, Mass., Jan. 1955.
3. G. Arnason, L. Vuorela: A Two-parameter Representation of the Normal Temperature Distribution of the 1000-500 mb layer. Tellus 7, 2, 1955.

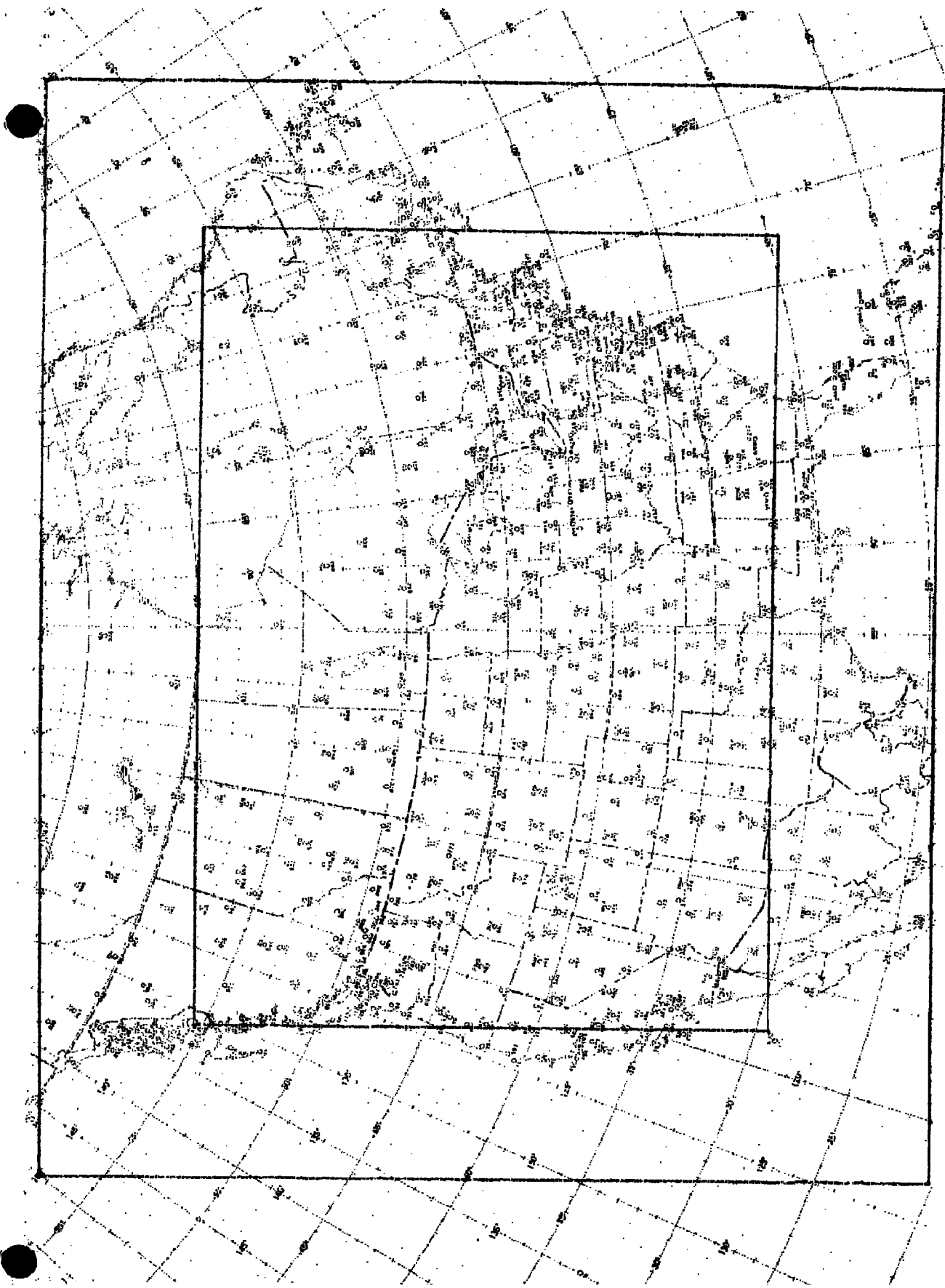


FIG. 1 THE GRID AND THE AREA OF VERIFICATION.

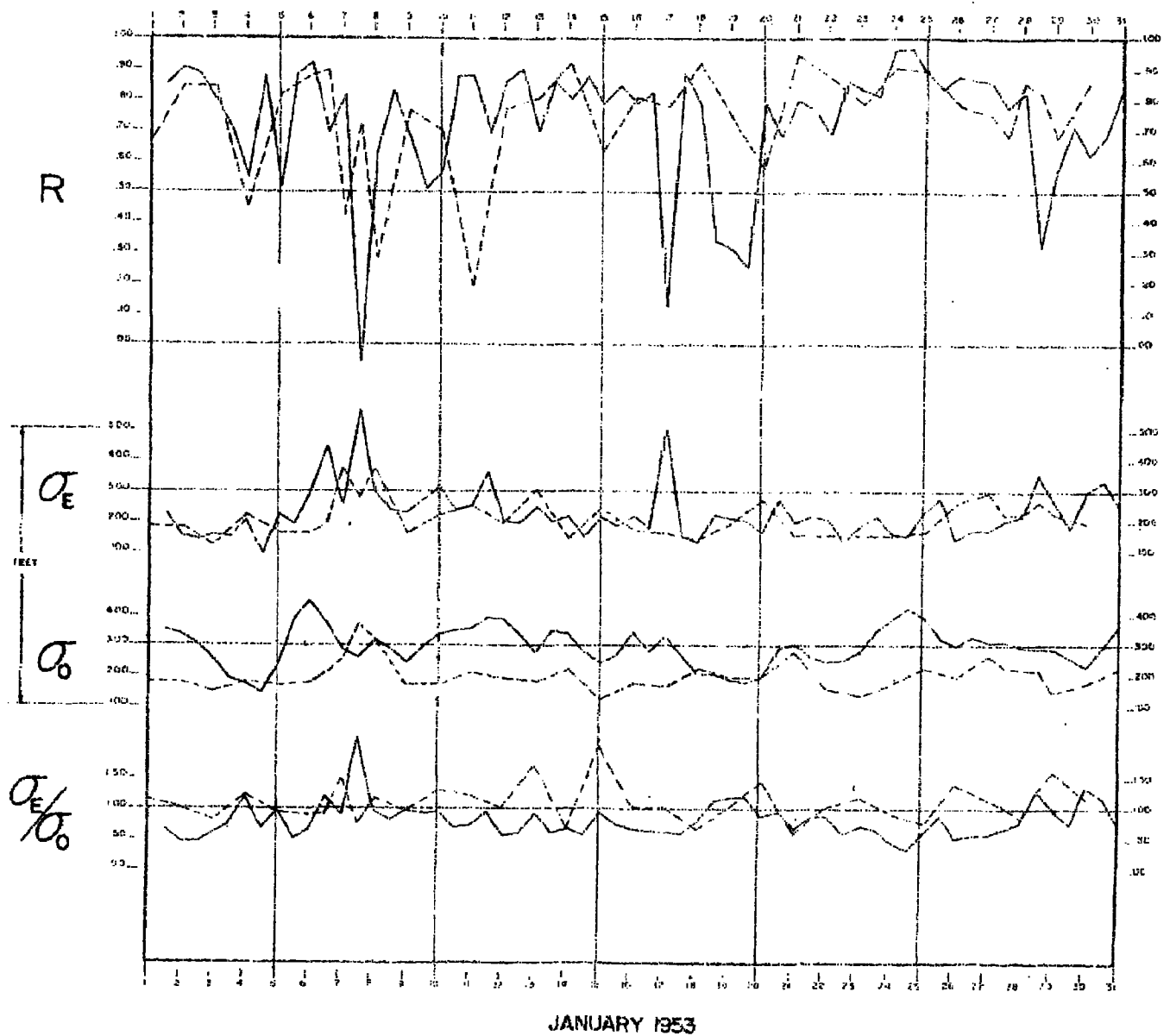


Fig. 2. R is the correlation coefficient, σ_E the root mean square of height errors, and σ_O the root mean square of observed height changes. Solid lines refer to the 500 mb and broken lines to the 100 mb forecasts

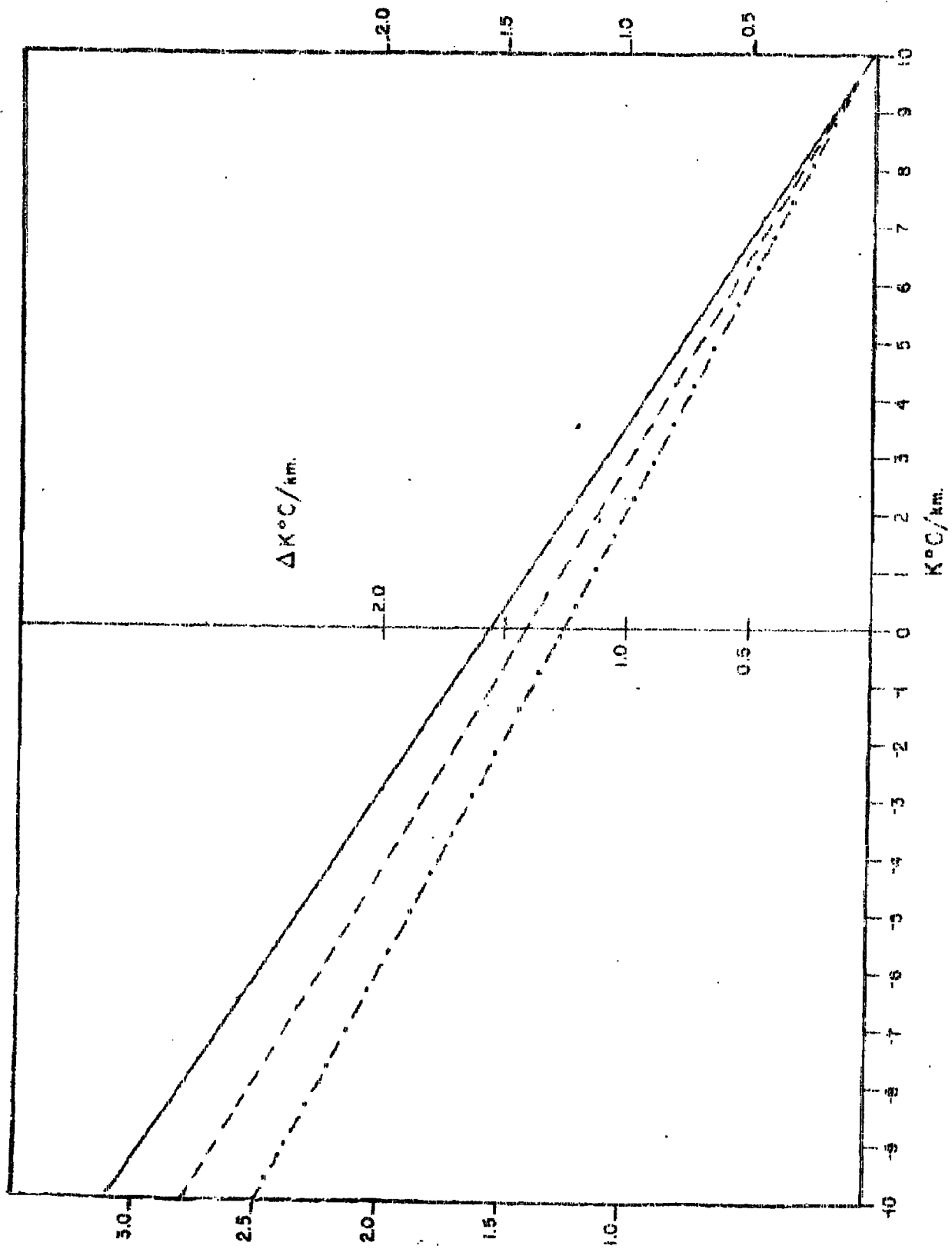


Fig. 3. The increase ΔK , as a function of K , required to make the last term in Eq. (4) zero. The solid, broken, and dash-dotted lines represent the lower, middle, and upper parts of the troposphere.